RESEARCH ARTICLE | APRIL 15 2024

Photonic crystal-coupled enhanced steering emission: A prism-free, objective-free, and metal-free loss-less approach for biosensing \odot

Seemesh Bhaskar 💿 ; Weinan Liu 💿 ; Joseph Tibbs 💿 ; Brian T. Cunningham 🗷 💿



Appl. Phys. Lett. 124, 161102 (2024) https://doi.org/10.1063/5.0203999









Photonic crystal-coupled enhanced steering emission: A prism-free, objective-free, and metal-free loss-less approach for biosensing (

Cite as: Appl. Phys. Lett. 124, 161102 (2024); doi: 10.1063/5.0203999 Submitted: 18 February 2024 · Accepted: 26 March 2024 · Published Online: 15 April 2024



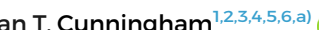








Seemesh Bhaskar, 1,2,3 (b) Weinan Liu, 1,2 (b) Joseph Tibbs, 2,4 (b) and Brian T. Cunningham 1,2,3,4,5,6,a) (b)







AFFILIATIONS

ABSTRACT

Diagnostic assays utilizing fluorescent reporters in the context of low abundance biomarkers for cancer and infectious disease can reach lower limits of detection through efficient collection of emitted photons into an optical sensor. In this work, we present the rational design, fabrication, and application of one-dimensional photonic crystal (PC) grating interfaces to accomplish a cost-effective prism-free, metal-free, and objective-free platform for augmentation of fluorescence emission collection efficiency. Guided mode resonance (GMR) of the PC is engineered to match the laser excitation (532 nm) and emission maximum (580 nm) of the radiating dipoles to arrive at optimized conditions. The photo-plasmonic hybrid nano-engineering using silver nanoparticles presented >110-fold steering fluorescence enhancement enabling placement of the sample between the excitation source and detector that are in a straight line. From the experimental and simulation inferences, we propose a radiating GMR model by scrutinizing the polarized emission properties of the hybrid substrate, in accordance with the radiating plasmon model. The augmented fluorescence intensity realized here with a simple detection instrument provides sub-nanomolar sensitivity to provide a path toward point-of-care scenarios.

Published under an exclusive license by AIP Publishing. https://doi.org/10.1063/5.0203999

Many current biosensing technologies that utilize fluorescent reporters require an optical microscopy setup in which an expensive objective is used to collect the fluorescence emission. 1-3 Photoplasmonic interfaces have been developed to augment the performance of such devices where the effective cost of the fluorescent detection instrument has been significantly reduced by using functional nanoengineering approaches and lower numerical aperture objectives. 4-6 In prior reports, we described the design, fabrication, and application of grating based photonic crystals (PCs) for photonic crystal enhanced fluorescence (PCEF), for applications that include cancer biomarker detection and infectious disease diagnostics.⁷⁻¹¹ There are many reports that utilize prism-dependent platforms to collect the highly directional fluorescence emission that, in turn, enhances the sensitivity of the instrument. 12-14 In the early 2000s, Lakowicz and co-workers proposed the radiating plasmon model where the radiating dipoles

excite the plasmons. 13,15 These excited plasmons radiate to the far-field by carrying the characteristics of the radiating dipoles (emission attribute) and the plasmons (polarization attribute). Following this revelation, numerous plasmonic metal thin film-based biosensing approaches have been established rendering high sensitivity due to significantly enhanced fluorescence. 16-18 However, the plasmonic metal thin film-based sensing platforms such as surface plasmon coupled emission (SPCE) suffer from two major drawbacks: (i) parasitic Ohmic losses in metal-containing structures and (ii) the critical role of the prism to achieve phase matching conditions in the generation of propagating plasmon polaritons. 19,20 In this Perspective, photonic crystal Bragg mirrors sustaining Bloch surface waves (BSWs) and internal optical modes (IOMs) were recently investigated in photonic crystal-coupled emission (PCCE) technology. 21-23 The utility of such all-dielectric interfaces has facilitated overcoming the first drawback,

 $^{^1}$ Department of Electrical and Computer Engineering, University of Illinois at Urbana-Champaign, Urbana, Illinois 61801, USA

²Nick Holonyak Jr., Micro and Nanotechnology Laboratory, University of Illinois at Urbana-Champaign, Urbana, Illinois 61801, USA

³Carl R. Woese Institute for Genomic Biology, University of Illinois at Urbana-Champaign, Urbana, Illinois 61801, USA

Department of Bioengineering, University of Illinois at Urbana-Champaign, Urbana, Illinois 61801, USA

⁵Department of Chemistry, University of Illinois at Urbana-Champaign, Urbana, Illinois 61801, USA

⁶Cancer Center at Illinois, Urbana, Illinois 61801, USA

a) Author to whom correspondence should be addressed: bcunning@illinois.edu

albeit at the expense of using a prism-dependent setup for biosensing applications. The critical unavoidable role of the prism in Kretschmann or reverse Kretschmann configuration arises from the dispersion properties of the metal thin films and Bragg mirrors. Highend fabrication and exorbitant methodologies dependent metal-dielectric-metal (MDM) and Tamm state-coupled emission (TSCE) configurations have been incorporated in the past not only to just overcome the dependence on the prism but also to realize the quintessential steering emission. Steering emission is a fluorescence output in which the optical setup is simplified and enables placement of the sample between the source and the detector in a straight line. We seek to achieve steering emission and to overcome existing limitations of the current methodologies.

In this work, we present an all-dielectric Bragg grating-based PC interface. The properties of the loss-less GMR are exploited to achieve unique steering fluorescence enhancements. While the prism-dependent SPCE and PCCE assist in obtaining directional (not steering) $\sim\!10\text{-fold}^{27}$ and $\sim\!40\text{-fold}^{28}$ fluorescence enhancement as compared to the glass interface, a $\sim\!25\text{-fold}$ enhancement in the "Photonic Crystal-coupled Enhanced Steering (PCES)" emission is demonstrated for identical conditions in a prism-free, metal-free, and objective-free setup. Furthermore, nano-engineering was incorporated to further augment the fluorescence intensity to $>\!110\text{-fold}$ using cavity-driven photo-plasmonic hotspots.

In order to accomplish direct comparisons, the conventionally used fluorescent reporter molecule, rhodamine B, was used as the radiating dipole in all the studies, with a 532 nm continuous wave (c.w.) laser, 550 nm long wave pass (LWP) filter, and a fiber optic (coupled to collimating lens) spectrometer (2000+) connected to Ocean Optics SpectraSuite software. All the PC substrates were cleaned with piranha solution (4:1 ratio of H₂SO₄ and H₂O₂ solutions) and rinsed with acetone, IPA, and Milli-Q® water before use. The radiating dipoles were interfaced over the PC substrate using a well-established spin coating method. 19,22,27 Two % PVA polymer spin-coated films applied at 3000 rpm for 1 minute yielded \sim 65 nm thin films (degree of hydrolysis 86%-89%; molecular weight 85 000-12 000 and 4000 g/mol). All the PC substrates for fluorescence measurements were fabricated by embedding the radiating dipoles in the polymer matrix and spin coating, followed by mounting on a calibrated 360° rotating stage, with optical configuration shown in Fig. 1(a). Simply put, from the SPR and SPCE point of view, the instrument can be visualized as a reverse Kretchmann (RK) configuration without a prism. 19,22,27 A scanning electron microscope (SEM) image of the parent PC (PC1) is shown in Fig. 1(b) along with its 3D atomic force microscope (AFM) profile. The AFM top view is presented in Fig. 1(c), along with the corresponding height profile in Fig. 1(d), demonstrating the depth of the grooves to be \sim 28 nm. The SEM images of all the three variants (PC₁, PC₂, and PC₃) are presented in Fig. S1.

Numerical simulations by rigorous coupled-wave analysis (RCWA) were performed to evaluate the thickness conditions for achieving the desired shift in the resonance of the PC. In order to accomplish tunable transmittance resonances, the parent PC₁ was initially sputter coated using TiO_2 and then spin coated with PVA dielectric [Figs. 1(e)-1(g)]. The 28 and 80 nm sputter coated PCs are referred to as PC₂ and PC₃ with the transmittance resonances for all the three variants shown in Fig. 1(h). Spin coating \sim 65 nm thin films of PVA dielectric over these substrates yielded resonance shifts as

shown in Fig. 1(i). The consistency in the PVA thickness analysis across all PC variants is presented in the supplementary material (Figs. S2-S4). These conditions are carefully chosen to comprehensively scrutinize the coupling characteristics of the radiating dipoles (embedded in PVA matrix) with the GMR of the underlying PCs. While the \sim 500 nm GMR of PC₁ serves as a substrate with a hypsochromic shift from the absorbance spectrum of the radiating dipole (also where the laser excitation is executed), the \sim 575 nm GMR of PC₃ serves as a variant for bathochromic shift from the absorption maximum and excitation laser line (Fig. 1). Although the PC2 presents the GMR at \sim 530 nm and exhibits ideal characteristics for PCCE on the account of excellent overlap between the laser excitation and dye's absorption, the experimental observations made in this work establish intriguing observations in line with the radiating surface wave model. 13,29 The transmittance of all the PC variants with and without PVA and input and output polarizers is discussed in the supplementary material (Figs. S5-S7). The spectral information of the white light used for all the transmittance measurements is also presented (Fig. S8).

The experimental fluorescence data for PC₃ are overlapped with the experimental transmittance spectra for unpolarized [Fig. 2(a)], TEpolarized [Fig. 2(b)], and TM-polarized [Fig. 2(c)] out-coupled light at 0° (the detector and laser are in straight line). We have chosen PC₃ for representation here because this particular variant engendered the highest fluorescence enhancements among all the three variants. From Figs. 2(a)-2(c), it is evident that there is an excellent overlap between the experimental transmittance and fluorescence spectra for all the polarizations. In other words, the emitted photons from the RhB radiating dipoles are out-coupled to the detector region via the allowed modes of the underlying substrate. Furthermore, the overlap of the experimental PCCE at different polarizations of out-coupled emission is presented in Fig. 2(d), highlighting the high polarization selectivity of the out-coupled emission. The numerically calculated dispersion diagram for PC3 is presented in Fig. 2(e), along with the overlap of the same with the experimental fluorescence data in Fig. 2(f) (the dispersion diagrams of experimental fluorescence and simulated results for PC₁, PC₂, and PC₃ for TE and TM polarizations are presented in Figs. S9-11). In addition to enabling 0° steering emission, PC₃ also demonstrates high fluorescence counts as compared to PC2 and PC1 [Fig. 2(g)]. The PCCE enhancements calculated as a direct ratio²² PCCE intensity counts to that of the fluorescence intensity counts over the glass substrate are shown in Fig. 2(h) along with the percentage polarization presented in Fig. 2(i), for all the three variants at optimum outcoupling angle. From the fluorescence intensity counts as well as the enhancements, it is clear that PC3 yielded highest fluorescence enhancements among the three variants.

These experimental results, supported by numerical calculations, present interesting inferences, namely: (i) engineering GMR of PC at wavelengths far from absorbance and emission spectra of radiating dipoles yields negligible fluorescence enhancements. (ii) Engineering the GMR of the PC exactly overlapping the laser line and the absorbance of radiating dipoles need not necessitate highest fluorescence enhancements. This is because the PC is not resonating at the emission wavelength of the radiating dipole. (iii) Although the GMR is not directly excited by the laser line in the PC₃ variant, the out-coupled steering emission is highly polarized with boosted fluorescence intensity, presenting highest fluorescence enhancements. This observation re-emphasizes the understanding that GMR of the PC need not be

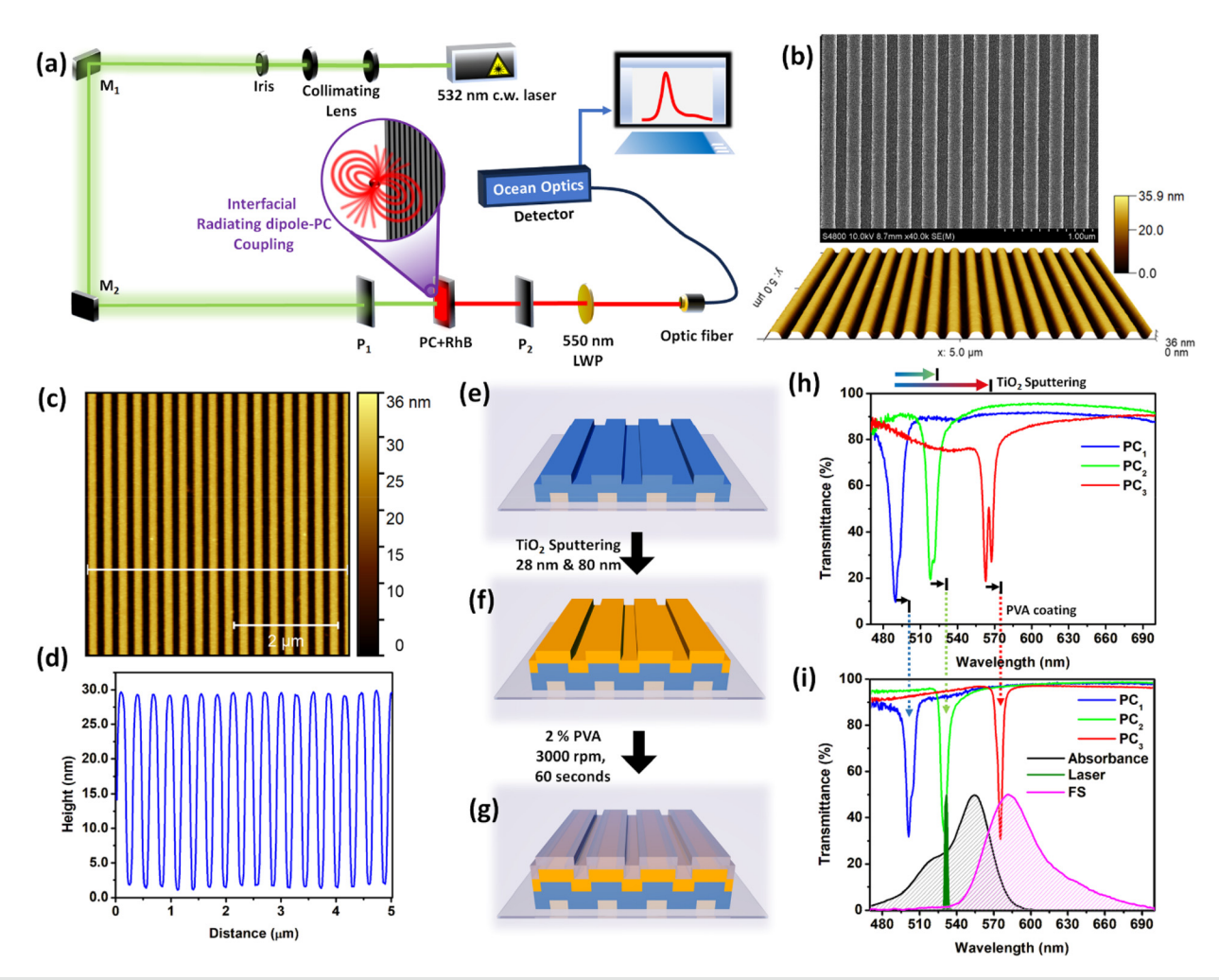


FIG. 1. Optical configuration and PC fabrication with electron microscopy, topography, and optical characterization. (a) Conceptual schematic of the optical setup used for PCCE experimentation. (b) SEM image of the parent photonic crystal (PC₁) shown along with the 3D AFM image. (c) AFM top view of the PC₁. (d) Height vs distance profile of the AFM line profile corresponding to (c). (e)–(g) Schematic of the modification of the PC with TiO₂ sputtering and PVA coating. Transmittance resonance dips of PC₁, PC₂, and PC₃, obtained (h) without PVA and (i) with PVA, where (i) captures the laser line, absorbance, and emission of RhB, all collected experimentally.

excited directly using a laser line in order to obtain augmented fluorescence, rather the emission from the radiating dipoles can accomplish this objective.^{2,13} Hence, as long as the radiating dipoles are excited by a suitable laser line and GMR of the PC matches the emission wavelength of the radiating dipoles, researchers can realize high fluorescence enhancements, in accordance with the radiating plasmon model.^{2,13,30,31} These intriguing experimental observations, thus, facilitate the proposition of the radiating GMR model, where we state (through observations made above) that the PCES emission can be realized with cost-effective platforms by tailoring the GMR of the grating-based PC to that of the emission wavelength of the radiating dipoles (excited at appropriate wavelengths), as emitted photons from the radiating dipoles, in turn, would excite the GMRs without requirement of direct laser excitation of GMR. Most importantly, the radiating dipoles not only carry their spectral signature to the far-field but also out-couple through the allowed modes of the PC, hence carrying the polarization selectivity of the underlying PC. Such observations render the radiating dipole-PC conjugate system as a hybrid radiating GMR platform. In other words, the photons captured by the detector in the far-field are not an independent functionality of radiating dipoles or PC disjointedly, but rather a hybrid manifestation of both of them, where the "radiating dipole-PC" system itself functions as a hybrid radiating entity. Although these observations are in accordance with the radiating surface wave model²⁹ and the radiating plasmon model, 2,13,30,31 it is worth noting that the radiating GMR model proposed in this work demonstrates a prism-free, objective-free, and a metal-free PCES emission technology. Furthermore, the additional details pertaining to different input and output polarization dependent fluorescence signal intensity and related discussions are presented in the supplementary material (Figs. S12 and S13). The PCCE enhancements and percentage polarization realized for all the variants at 0° are discussed in the supplementary material (Fig. S14).

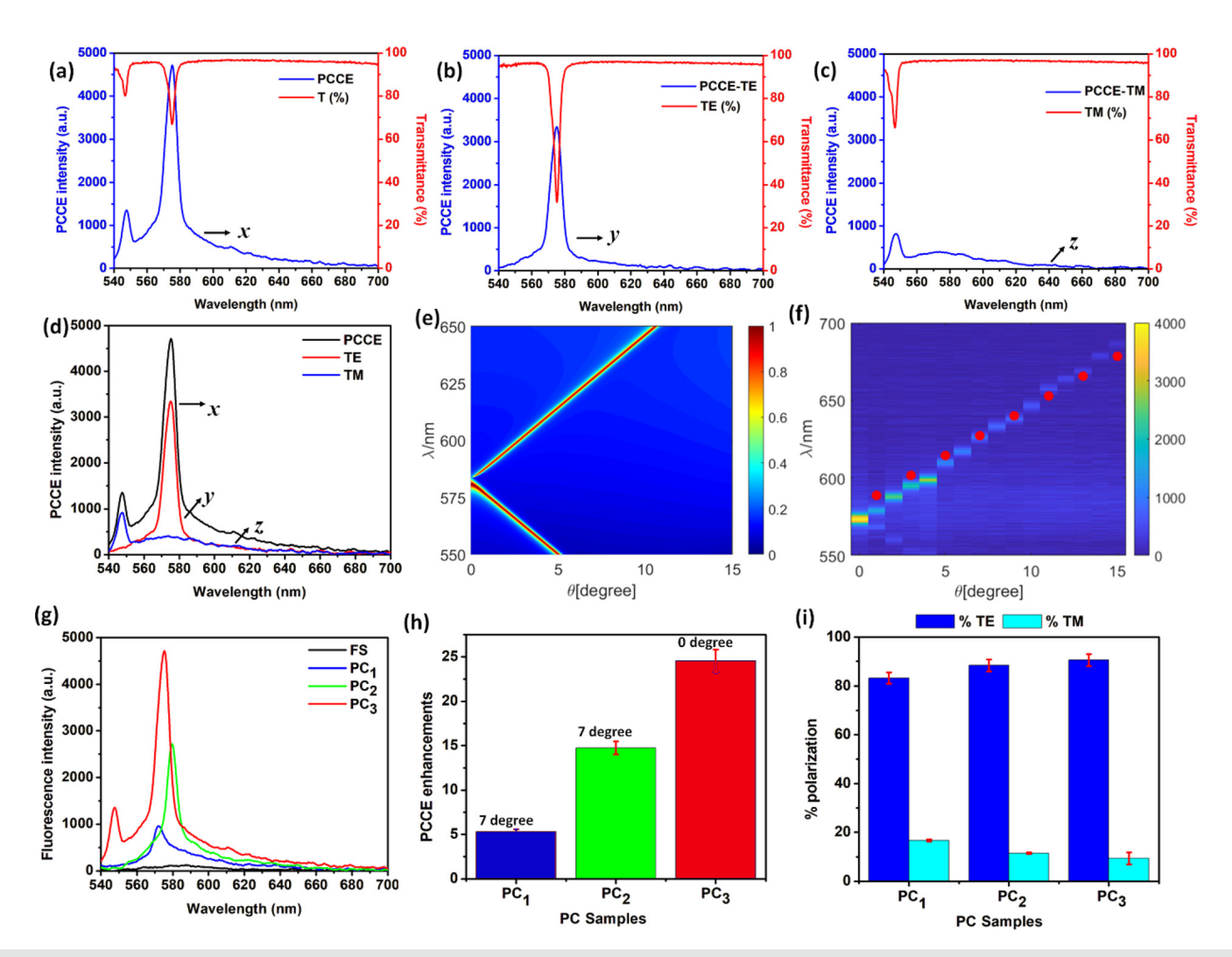


FIG. 2. Experimental and theoretical analysis of fluorescence coupling with PC, enhancements, and polarization. (a) Unpolarized, (b) TE polarized, and (c) TM-polarized transmittance spectra of PC₃ overlapped with the corresponding PCCE intensity profiles. (d) Overlap of unpolarized, TE-, and TM-polarized out-coupled PCCE intensity. (e) Computer simulated dispersion diagram of PC₃. (f) Overlap of computed dispersion diagram (shown as red dots) with the experimental fluorescence spectra (shown as shaded region). (g) Fluorescence intensity spectra, (h) PCCE enhancements, and (i) percentage polarization obtained at optimum outcoupling angle for all three variants under investigation, PC₁, PC₂, and PC₃.

Furthermore, scientists in the domain of fluorescence spectroscopy incorporate numerous approaches to amplify the fluorescence emission intensity. The two most widely adopted techniques are: (i) use of myriad optical elements such as focusing lens, prisms, and conical mirrors in different configurations to improve the overall collection efficiency, albeit at the expense of incorporating exorbitant optical elements, and (ii) the use of effective nano-engineering approaches to substantially enhance the photo-plasmonic coupling efficiency at the micro-nano-interface of different platforms. 19,27,32 The second approach not only renders a cost-effective means to develop a biosensing framework but also supports mass scale production of devices, especially on the account of the nano-entities utilized that present high surface-to-volume ratio and robust performance. Cao and co-workers have explored several such approaches incorporating spacer, cavity, and extended cavity nanointerfaces in SPCE and PCCE platforms.¹ Our laboratory reported the use of grating-based PCs to realize boosted fluorescence enhancements for the detection of cancer biomarkers. 4,

In this background, to further improve the out-coupled fluorescence signal intensity, we present the viability of cavity nano-engineering where the freshly prepared AgNPs (1 μg ml $^{-1}$) are admixed with PVA and radiating dipoles, and spin coated over the PC surface. ^{19,28,33}

The absorbance spectra [Fig. 3(a)], TEM, HRTEM [Fig. 3(b)], and SAED [Fig. 3(c)] of the synthesized AgNPs are comprehensively analyzed to validate the synthesis methodology (supplementary material, p. S16). Such cavity nanointerface generates myriad regions of infinitesimal nanogaps between the PC and the AgNPs, where the radiating dipoles get interfaced. ^{19,27,31} Such nano-regimes experience high electric field intensity on the account of the hybridized modes from localized surface plasmon resonance (LSPR) of AgNPs and the counter-propagating GMR based evanescent field of the underlying PC. ^{3,27} Consequently, the PCCE enhancements increase from ~25-fold to ~110-fold with concomitant reduction in the lifetime of the radiating dipoles (Fig. S15). While the RhB over glass presented monoexponential decay with a lifetime of 3.58 ns, ^{20,23,32} interfacing the

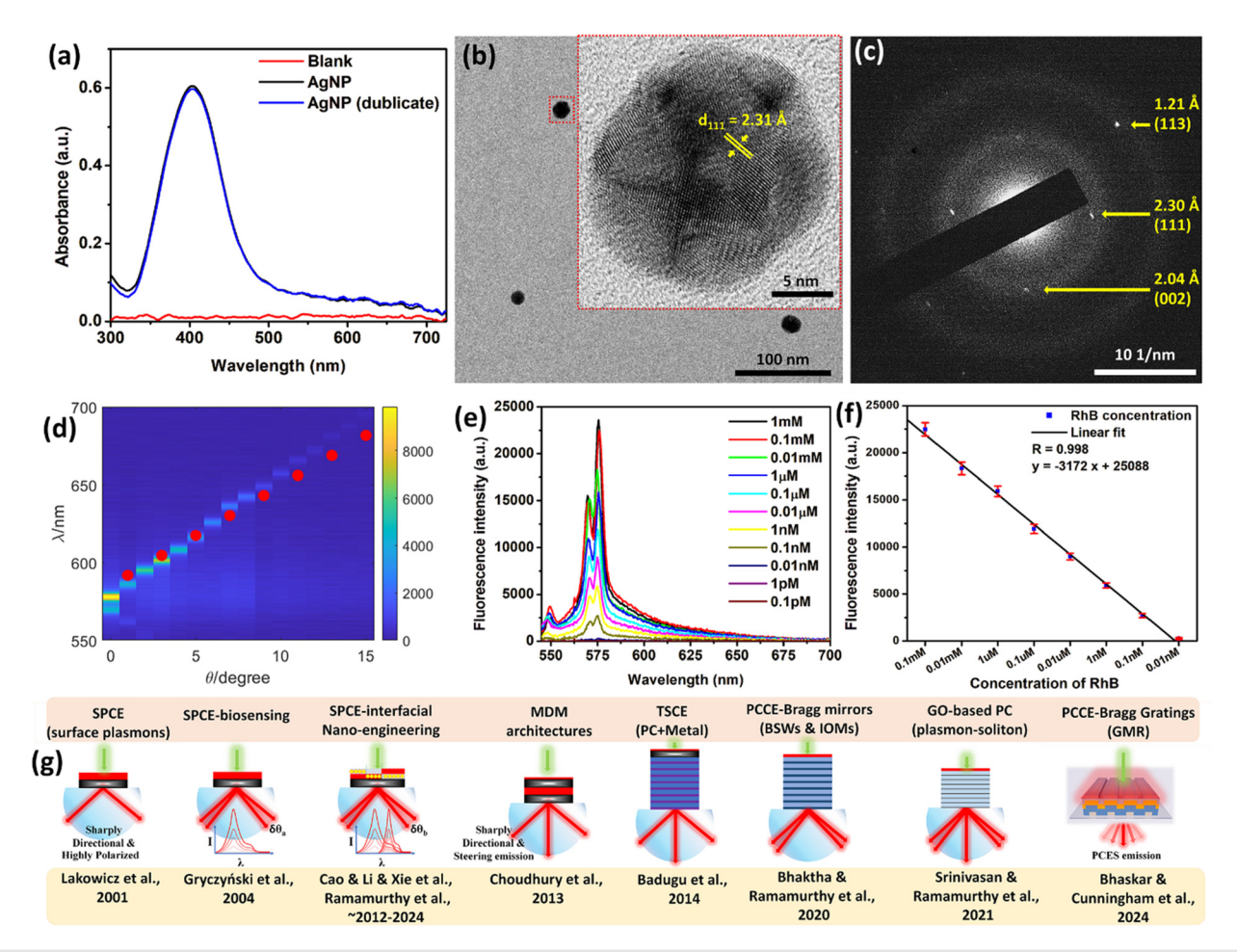


FIG. 3. Nano-engineering plasmonic AgNPs over PCCE substrate for picomolar RhB sensing. (a) Absorbance spectra of AgNPs in duplicates and blank (Milli- Q^{\odot} water). (b) TEM image of AgNPs shown with the HRTEM depicting the characteristic lattice fringes of Ag. (c) SAED of AgNPs. (d) Overlap of the numerically calculated dispersion diagram for PC₃ (shown as dotted red line) with that of the experimentally obtained fluorescence intensity (shown as shaded region). (e) Fluorescence intensity spectra and (f) intensity counts from PCCE incorporating AgNPs, for the detection of RhB molecules at different concentrations. (g) Conceptual schematic of the development of biosensing platforms based on fluorescence spectroscopy spanning the past \sim 20 years.

same over the PC and with AgNPs+PC hybrid yielded monoexponential 2.05 ns and biexponential lifetime contributions (0.14 ns, 67.5% and 2.65 ns, 32.5%), respectively. Hence, we envisage a high radiative decay rate facilitated by the judicious synergy of plasmonic AgNPs and ³² Importantly, while metal-dependent SPCE platunderlying PC.20 form renders ~10-fold and ~60-fold for blank and AgNPs-cavity interface, respectively, this Letter experimentally validates the preeminence of metal-free, loss-less PC based platform for realization of ~25-fold and >110-fold PCCE enhancements under identical conditions. The excellent overlap between the numerically calculated and experimentally obtained dispersion diagrams is presented in Fig. 3(d). In order to verify the relevance and robustness of the subject platform for biosensing applications, the typical SPCE and PCCE reporter molecule, RhB, was studied in the hybrid nanocavity interface at different concentrations ranging from 1 mM to 0.1 pM [Fig. 3(e)]. The platform demonstrates a large linear sensing regime from 0.1 mM to 0.01 nM with high sensitivity estimated as the slope (3172/dec) and \sim 10 pM

limit of detection, with high reproducibility (standard deviation presented for triplicate measurements) [Fig. 3(f)].

The major breakthroughs in the plasmon-controlled fluorescence spectroscopy are summarized conceptually in Fig. 3(g). Following the cogent observations and reports of radiative decay engineering series 1–8 by Lakowicz and co-workers, 35–37 a plethora of innovations especially associated with MDM, 24,25 TSCE, 26 SPCE, 19,38 PCCE, 21,23 and graphene oxide 39 based biosensing platforms have been documented and succinctly captured in Fig. 3(g). The current report demonstrates the robustness of a highly desirable approach using photo-plasmonic dielectric-metal hybrid interface for augmenting the fluorescence signal intensity. In the case of adjacently situated plasmonic NPs and radiating dipoles, the radiation pattern and intensity of the fluorescence are significantly modulated by the plasmonic NPs. Consequently, the system has been justifiably addressed as plasmophore (plasmon+fluorophore) as the radiation in the far-field renders photons that carry the characteristic information of both the plasmons and the radiating dipoles. 2,13,30,31

In this scenario, the emitted photons from the excited radiating dipoles are coupled to the LSPR of AgNPs and GMR of PC, thereby resulting in a coherent and collective photo-plasmonic coupling efficiency. In other words, while the AgNPs by themselves foster PCF (through generation of plasmophore) via occurrence of radiating plasmon, the GMR of the PC presents augmented and highly polarized fluorescence signal intensity via the radiating GMR model. Hence, this report presents a comprehensive understanding of nano-engineering at PC interface, highlighting the advantages it offers to synergistically understand the physicochemical interactions of numerous nanomaterials such as ferromagnetic, ferrielectric, piezoelectric, transition metal, lanthanide oxides, and low-dimensional substrates (0D, 1D, and 2D), to name a few from the perspective of futuristic scope of the work (outlined in Fig. S16). Such exploration would not only present valuable insights to the optoelectronic community but also engender the development of myriad PCES emission biosensing frameworks for the detection of molecular biomarkers and environmentally relevant hazardous analytes.

In the development of biosensing technologies, there is always a quintessential requirement to constantly upgrade the performance of the device with respect to sensitivity, reproducibility, and robustness. Recently, awareness toward simplifying the optical detection technologies has been garnering tremendous importance from sustainable mass scale production perspective vis-à-vis the scientific rigor-propelled discipline-driven exploration of cumbersome, exorbitant, and non-user-friendly platforms that render unprecedented performance. In this context, this Letter presents an effective nano-engineering method to generate hybrid radiating GMR platforms, demonstrating high fluorescence enhancement and polarization selectivity enabling quantitative analysis via reliable and reproducible picomolar limit of detection of target analyte. Our approach supports the development of early diagnostic tools, especially in the point-of-care domain catering to the needs of resource-scarce settings.

See the supplementary material for details on comprehensive characterization of the substrates under investigation, using AFM, SEM, FIB-SEM, and TEM; transmittance measurements; and lifetime analysis. The dispersion diagrams obtained via simulations and experimental fluorescence for all the three variants of PC (PC₁, PC₂, and PC₃) is discussed for TM and TE polarizations of light. The free space (FS), PCCE intensity analysis and the transmittance data analysis under different input and output polarizations (TM and TE) of light are discussed. The scope and perspectives of the current research are outlined, presenting opportunities for future work in this direction.

The authors gratefully acknowledge funding from the National Institutes of Health (Nos. R01AI159454, R01CA227699, R01AI139401, R01EB029805, and RadXRad Program Grant No. U01AA029348) and the National Science Foundation (NSF RAPID 20-27778, CBET 19-00277, and CBET 22-32681). Financial support was also provided by the Cancer Center at Illinois. J.T. is supported by the Illinois Distinguished Fellowship and the National Science Foundation graduate research fellowship. S.B. is supported by a postdoctoral fellowship from the Carl R. Woese Institute for Genomic Biology. S.B. thanks the research scientists Elbashir Araud, Kathy Walsh, Ying He, Wacek Swiech, Honghui Zhou, Julio Antonio Nieri D. Soares, Duncan Nall, Umnia Doha, and Glenn Fried for their support and research inputs in characterization of materials. The support from the IGB Core Facilities,

instruments including WITec Alpha 300 RA Raman-AFM-SNOM and Confocal-Zeiss LSM 710-Multiphoton Microscope, as well as the Clean room facility and BioNanotechnology Laboratory (BNL) at HMNTL and the associated research scientists are gratefully acknowledged. The support from the instruments Asylum Research MFP-3D AFM; Hitachi S-4800 High Resolution SEM; Au-Pd Sputter Coater - Emscope SC 500; FEI Helios 600i Dual Beam SEM/FIB; Time-Resolved Photoluminescence, Sensitivity: single photon, Room temperature and 77 K; 532 nm laser excitation; and JEOL 2100 CRYO TEM, the associated staff and research scientists at Materials Research Laboratory, The Grainger College of Engineering, UIUC is gratefully acknowledged. The authors thank the feedback provided by all the members of the Nanosensors group, HMNTL, during scientific discussions.

AUTHOR DECLARATIONS

Conflict of Interest

The authors have no conflicts to disclose.

Author Contributions

Weinan Liu and Joseph Tibbs contributed equally to this work.

Seemesh Bhaskar: Conceptualization (lead); Data curation (equal); Formal analysis (lead); Funding acquisition (equal); Investigation (lead); Methodology (equal); Software (equal); Validation (equal); Visualization (lead); Writing – original draft (lead); Writing – review & editing (equal). Weinan Liu: Data curation (equal); Formal analysis (equal); Investigation (equal); Methodology (equal); Software (equal); Validation (equal); Writing – review & editing (supporting). Joseph Tibbs: Data curation (equal); Formal analysis (equal); Investigation (equal); Methodology (equal); Software (equal); Validation (equal); Writing – review & editing (supporting). Brian T. Cunningham: Funding acquisition (lead); Project administration (lead); Resources (lead); Supervision (lead); Validation (lead); Writing – review & editing (lead).

DATA AVAILABILITY

The data that support the findings of this study are available from the corresponding author upon reasonable request.

REFERENCES

- ¹A. Pokhriyal, M. Lu, C. S. Huang, S. Schulz, and B. T. Cunningham, "Multicolor fluorescence enhancement from a photonics crystal surface," Appl. Phys. Lett. **97**(12), 121108 (2010).
- ²J. R. Lakowicz, "Plasmonics in biology and plasmon-controlled fluorescence," Plasmonics 1(1), 5–33 (2006).
- ³N. Ganesh, W. Zhang, P. C. Mathias, E. Chow, J. A N. T. Soares, V. Malyarchuk, A. D. Smith, and B. T. Cunningham, "Enhanced fluorescence emission from quantum dots on a photonic crystal surface," Nat. Nanotechnol. 2(8), 515–520 (2007).
- ⁴C.-S. Huang, S. George, M. Lu, V. Chaudhery, R. Tan, R. C. Zangar, and B. T. Cunningham, "Application of photonic crystal enhanced fluorescence to cancer biomarker microarrays," Anal. Chem. 83(4), 1425–1430 (2011).
- ⁵A. Pokhriyal, M. Lu, V. Chaudhery, C.-S. Huang, S. Schulz, and B. T. Cunningham, "Photonic crystal enhanced fluorescence using a quartz substrate to reduce limits of detection," Opt. Express 18(24), 24793–24808 (2010).
- ⁶Principles of Fluorescence Spectroscopy, edited by Lakowicz, J. R. (Springer, Boston, MA, 2006).

- ⁷P. C. Mathias, N. Ganesh, L. L. Chan, and B. T. Cunningham, "Combined enhanced fluorescence and label-free biomolecular detection with a photonic crystal surface," Appl. Opt. 46(12), 2351–2360 (2007).
- ⁸W. Zhang, N. Ganesh, P. C. Mathias, and B. T. Cunningham, "Enhanced fluorescence on a photonic crystal surface incorporating nanorod structures," Small 4(12), 2199–2203 (2008).
- ⁹P. C. Mathias, H.-Y. Wu, and B. T. Cunningham, "Employing two distinct photonic crystal resonances to improve fluorescence enhancement," Appl. Phys. Lett. 95(2), 021111 (2009).
- ¹⁰W. Chen, K. D. Long, H. Yu, Y. Tan, J. Sun Choi, B. A. Harley, and B. T. Cunningham, "Enhanced live cell imaging via photonic crystal enhanced fluorescence microscopy," Analyst 139(22), 5954–5963 (2014).
- ¹¹A. Pokhriyal, M. Lu, V. Chaudhery, S. George, and B. T. Cunningham, "Enhanced fluorescence emission using a photonic crystal coupled to an optical cavity," Appl. Phys. Lett. 102(22), 221114 (2013).
- ¹²S. Dutta Choudhury, R. Badugu, and J. R. Lakowicz, "Directing fluorescence with plasmonic and photonic structures," Acc. Chem. Res. 48(8), 2171–2180 (2015).
- ¹³J. R. Lakowicz, K. Ray, M. Chowdhury, H. Szmacinski, Y. Fu, J. Zhang, and K. Nowaczyk, "Plasmon-controlled fluorescence: A new paradigm in fluorescence spectroscopy," Analyst 133(10), 1308–1346 (2008).
- ¹⁴T. Ming, H. Chen, R. Jiang, Q. Li, and J. Wang, "Plasmon-controlled fluorescence: Beyond the intensity enhancement," J. Phys. Chem. Lett. 3(2), 191–202 (2012).
- (2012). ¹⁵J. R. Lakowicz, "Radiative decay engineering 5: Metal-enhanced fluorescence and plasmon emission," Anal. Biochem. **337**(2), 171–194 (2005).
- ¹⁶S.-H. Cao, W.-P. Cai, Q. Liu, and Y.-Q. Li, "Surface plasmon-coupled emission: What can directional fluorescence bring to the analytical sciences?," Annu. Rev. Anal. Chem. 5(1), 317–336 (2012).
- ¹⁷M. Chen, S.-H. Cao, and Y.-Q. Li, "Surface plasmon-coupled emission imaging for biological applications," Anal. Bioanal. Chem. 412(24), 6085–6100 (2020).
- 18 V. S. K. Cheerala, K. M. Ganesh, S. Bhaskar, S. S. Ramamurthy, and S. C. Neelakantan, "Smartphone-based attomolar cyanide ion sensing using Au-graphene oxide cryosoret nanoassembly and benzoxazolium-based fluorophore in a surface plasmon-coupled enhanced fluorescence interface," Langmuir 39, 7939 (2023).
- ¹⁹D. Thacharakkal, S. Bhaskar, T. Sharma, G. Rajaraman, S. Sathish Ramamurthy, and C. Subramaniam, "Plasmonic synergism in tailored metalcarbon interfaces for real-time single molecular level sniffing of PFOS and PFOA," Chem. Eng. J 480, 148166 (2024).
- ²⁰S. Bhaskar, D. Thacharakkal, S. S. Ramamurthy, and C. Subramaniam, "Metal-dielectric interfacial engineering with mesoporous nano-carbon florets for 1000-fold fluorescence enhancements: Smartphone-enabled visual detection of perindopril erbumine at a single-molecular level," ACS Sustainable Chem. Eng. 11(1), 78–91 (2023).
- ²¹S. Bhaskar, P. Das, V. Srinivasan, S. Bhaktha B. N, and S. S. Ramamurthy, "Bloch surface waves and internal optical modes-driven photonic crystalcoupled emission platform for femtomolar detection of aluminum ions," J. Phys. Chem. C 124(13), 7341–7352 (2020).
- ²²S. Bhaskar, A. K. Singh, P. Das, P. Jana, S. Kanvah, B. N. Shivakiran Bhaktha, and S. S. Ramamurthy, "Superior resonant nanocavities engineering on the photonic crystal-coupled emission platform for the detection of femtomolar iodide and zeptomolar cortisol," ACS Appl. Mater. Interfaces 12(30), 34323–34336 (2020).
- 23S. Sudha Maria Lis, S. Bhaskar, R. Dahiwadkar, S. Kanvah, S. S. Ramamurthy, and B. N. Shivakiran Bhaktha, "Plasmon-rich BCZT nanoparticles in the photonic crystal-coupled emission platform for cavity hotspot-driven attomolar sensing," ACS Appl. Nano Mater. 6(20), 19312–19326 (2023).

- ²⁴S. Dutta Choudhury, R. Badugu, K. Nowaczyk, K. Ray, and J. R. Lakowicz, "Tuning fluorescence direction with plasmonic metal-dielectric-metal substrates," J. Phys. Chem. Lett. 4(1), 227–232 (2013).
- 25S. Dutta Choudhury, R. Badugu, K. Ray, and J. R. Lakowicz, "Steering fluorescence emission with metal-dielectric-metal structures of Au, Ag, and Al," J. Phys. Chem. C 117(30), 15798–15807 (2013).
- 26R. Badugu, E. Descrovi, and J. R. Lakowicz, "Radiative decay engineering 7: Tamm state-coupled emission using a hybrid plasmonic-photonic structure," Anal. Biochem. 445, 1-13 (2014).
- ²⁷A. Rai, S. Bhaskar, K. M. Ganesh, and S. S. Ramamurthy, "Hottest hotspots from the coldest cold: Welcome to nano 4.0," ACS Appl. Nano Mater. 5(9), 12245–12264 (2022).
- 28S. Bhaskar, S. Sudha Maria Lis, S. Kanvah, B. N. Shivakiran Bhaktha, and S. S. Ramamurthy, "Single-molecule cholesterol sensing by integrating silver nanowire propagating plasmons and graphene oxide π-plasmons on a photonic crystal-coupled emission platform," ACS Appl. Opt. Mater. 1(1), 159–172 (2023).
- ²⁹S. Bhaskar, P. Das, V. Srinivasan, B. N. Shivakiran Bhaktha, and S. S. Ramamurthy, "Plasmonic-silver sorets and dielectric-Nd₂O₃ nanorods for ultrasensitive photonic crystal-coupled emission," Mater. Res. Bull 145, 111558 (2022).
- ³⁰K. Aslan, Z. Leonenko, J. R. Lakowicz, and C. D. Geddes, "Annealed silverisland films for applications in metal-enhanced fluorescence: Interpretation in terms of radiating plasmons," J. Fluoresc. 15(5), 643–654 (2005).
- ³¹K. M. Ganesh, S. Bhaskar, V. S. K. Cheerala, P. Battampara, R. Reddy, S. C. Neelakantan, N. Reddy, and S. S. Ramamurthy, "Review of gold nanoparticles in surface plasmon-coupled emission technology: Effect of shape, hollow nanostructures, nano-assembly, metal-dielectric and heterometallic nanohybrids," Nanomaterials 14(1), 111 (2024).
- ³²S. Bhaskar, V. Srinivasan, and S. S. Ramamurthy, "Nd₂O₃-Ag nanostructures for plasmonic biosensing, antimicrobial, and anticancer applications," ACS Appl. Nano Mater. 6(2), 1129–1145 (2023).
- ³³ A. Rai, S. Bhaskar, N. Reddy, and S. S. Ramamurthy, "Cellphone-aided attomolar zinc ion detection using silkworm protein-based nanointerface engineering in a plasmon-coupled dequenched emission platform," ACS Sustainable Chem. Eng. 9(44), 14959–14974 (2021).
- 34P. Barya, Y. Xiong, S. Shepherd, R. Gupta, L. D. Akin, J. Tibbs, H. K. Lee, S. Singamaneni, and B. T. Cunningham, "Photonic-plasmonic coupling enhanced fluorescence enabling digital-resolution ultrasensitive protein detection," bioRxiv (2022).
- 35I. Gryczynski, J. Malicka, Z. Gryczynski, and J. R. Lakowicz, "Radiative decay engineering 4. Experimental studies of surface plasmon-coupled directional emission," Anal. Biochem. 324(2), 170–182 (2004).
- 36L. Zhu, R. Badugu, D. Zhang, R. Wang, E. Descrovi, and J. R. Lakowicz, "Radiative decay engineering 8: Coupled emission microscopy for lensfree high-throughput fluorescence detection," Anal. Biochem. 531, 20–36 (2017)
- ³⁷Z. Gryczynski, I. Gryczynski, E. Matveeva, J. Malicka, K. Nowaczyk, and J. R. Lakowicz, "Surface-plasmon-coupled emission: New technology for studying molecular processes," in *Cytometry: New Developments, Methods in Cell Biology*, 4th ed. (Academic Press, 2004), Vol. 75, pp 73–104.
- ³⁸J. R. Lakowicz, "Radiative decay engineering: biophysical and biomedical applications," Anal. Biochem. 298(1), 1–24 (2001).
- ³⁹S. Bhaskar, N. S. Visweswar Kambhampati, K. M. Ganesh, P. Mahesh Sharma, V. Srinivasan, and S. S. Ramamurthy, "Metal-free, graphene oxide-based tunable soliton and plasmon engineering for biosensing applications," ACS Appl. Mater. Interfaces 13(14), 17046–17061 (2021).